Structures and Properties of Ubiquinone-1 and Its Radical Anion from Hybrid Hartree−Fock/Density Functional Studies[1]

Scott E. Boesch and Ralph A. Wheeler*

Department of Chemistry and Biochemistry, University of Oklahoma, 620 Parrington Oval, Room 208, Norman, Oklahoma 73019

Received: February 17, 1997; In Final Form: May 28, 1997[⊗]

Ubiquinones and their semiquinone radical anions—electron transfer cofactors vital for respiration and photosynthesis—are typically characterized in proteins by measuring their vibrational or electron spin resonance spectra. This contribution presents calculated geometries and spin properties for ubiquinone-1 (UQ_1) and its radical anion ($UQ_1^{\bullet-}$), as well as vibrational frequencies for a model with the methyl groups on the isoprenyl side chain of UQ_1 replaced by hydrogens (UQ and $UQ^{\bullet}$). Computations were done by using the hybrid Hartree−Fock/density functional B3LYP method with the 6-31G(d) and [632|41] basis sets. Bond distance changes upon reducing UQ_1 to $UQ_1^{\bullet-}$ are qualitatively consistent with results for other *p*-benzoquinones. Proton and ^{13}C hyperfine coupling constants calculated by using Chipman's [632|41] basis set agree exceptionally well with experimental measurements and reflect the distribution of unpaired spin. We suggest isotopic substitution experiments to resolve the nearly overlapping C═O and C═C stretching frequencies calculated for UQ and to shift methoxy and/or methyl CH bending modes away from one CO stretching band of $UQ^{\bullet-}$.

Introduction

Ubiquinones-*n* or coenzymes Q (abbreviated UQ_n, $n = 6-10$, and shown in **1**) are vital redox cofactors in energy storage by photosynthesis and energy utilization by respiration.[2−7] In the bacterium *Rhodobacter sphaeroides*, for example, a primary ubiquinone is reduced to its semiquinone radical anion ($UQ_{10}^{\bullet-}$, the singly reduced form of **1** with $n = 10$) and subsequently passes the electron to a second ubiquinone.[4,5] In respiration, the reverse reaction, the oxidation of ubisemiquinone radical anions is also a key step.[6,7] In addition, the facile redox chemistry of ubiquinones is exploited by administering them as nutritional supplements for their antioxidant and radical scavenging properties.[8]

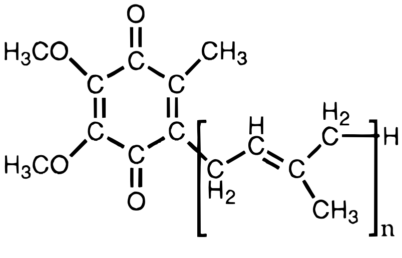

1

Ubiquinones-n

Despite their biochemical importance, experimental data for free ubiquinones and their semiquinone radical anions are limited. Although X-ray diffraction studies have been accomplished to determine the structures of ubiquinones bound in the photosynthetic reaction center,[9−14] the structure of free ubiquinone-1 was only recently predicted,[15] and the structure of ubiquinone radical anions must be inferred indirectly from measured spectra.[16−18] Experimental spectroscopic data for free ubiquinones and their radical anions are limited to several experimental vibrational frequencies,[16,19−24] hyperfine coupling constants, and spin densities for ubisemiquinone radical anions.[18,25−28] Yet measured vibrational and magnetic resonance spectra for the free species are vital for making structural inferences about protein-bound quinones or semiquinone anions. For example, shifts in measured CO stretching frequencies relative to free ubiquinones/semiquinone anions are usually taken to indicate some hydrogen bonding between the protein and a quinone's or semiquinone anion's oxygen atoms.[16,17] In addition, the effects of hydrogen bonding and other cofactors in the photosynthetic reaction center (such as a nearby iron atom) on spin densities and measured hyperfine coupling constants for ubqisemiquinone radical anions are currently being probed.[18] A firm, fundamental knowledge of vibrational frequencies, their corresponding vibrational modes, hyperfine coupling constants, and spin densities for free ubiquinones and their radical anions is therefore critical for valid comparisons with spectra of the protein-bound species. This computational study seeks to fill these gaps in our knowledge of ubiquinones and their semiquinone radical anions. We therefore compare the predicted structures of ubisemiquinone radical anions, their spin properties, vibrational frequencies, and corresponding vibrational modes with those of ubiquinones. For computational economy, some calculations were performed for the model compound UQ, shown in **2**, that differs from UQ_1 (**1** with $n = 1$) only in the replacement of the isoprenyl chain's methyl groups by hydrogens. This study uses the B3LYP hybrid Hartree−Fock/density functional method,[29,30] whose general features and advantages for this study are described in some detail next, in the section "Computational Methods".

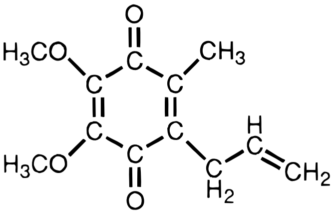

2

UQ model

[⊗] Abstract published in *Advance ACS Abstracts,* July 15, 1997.

S1089-5639(97)00584-7 CCC: $14.00

Computational Methods

Optimum geometries and their energies for UQ_0, UQ_1, and $UQ_1^{\bullet-}$ were calculated using the B3LYP/6-31G(d) hybrid Hartree–Fock/density functional method,[29] with the GAUSSIAN94 computer programs.[30] To calculate a minimum energy orientation of the isoprenyl side chain, we performed optimizations from six noneclipsed starting conformations of the chain for the neutral and anionic forms. Three energy minima for the dihedral angle about the central C–C bond of the isoprenyl chain were found at 2.1°, 250°, and 121.0°, with the latter angle having the lowest energy. The same procedure led to similar results for the radical anion, whose lowest energy isoprenyl chain conformation has a dihedral angle of 123°. Isotropic hyperfine coupling constants are proportional to spin densities at the nuclei[31,32] and were calculated from Fermi contact spin densities, whereas atomic spin densities were calculated by using Mulliken population analysis.[33] Spin densities are therefore only qualitatively correct. Isotropic hyperfine coupling constants using Chipman's [632|41] basis set were calculated at B3LYP/6-31G(d) geometries. Vibrational frequencies were calculated by using the smaller 6-31G(d) basis set, geometries optimized using the same basis set, and model compounds with hydrogens replacing the isoprenyl methyls of ubiquinones (UQ and $UQ^{\bullet-}$). Supporting Information demonstrates the close agreement between calculated geometries for $UQ/UQ^{\bullet-}$ and $UQ_1/UQ_1^{\bullet-}$. Mode assignments were performed by calculating total energy distributions[34] using the GAMESS[35,36] quantum chemistry program and by animating each mode using the program XMOL.[37]

Structures and Properties of Ubiquinones and Their Radical Anions

To our knowledge, no experimental structure is published for any free ubiquinone, so we compare calculated and published X-ray diffraction[38] bond distances and methoxy torsional angles for UQ_0, a ubiquinone analog lacking the isoprenyl chain (**1** with $n = 0$, abbreviated UQ_0). We note that an experimental structure for a 2,3-dimethoxy-5-prenyl-*p*-benzoquinone has also been published, but decomposition of the crystal hindered highly accurate determination of bond distances.[39] Experimental and calculated bond distances for UQ_0 shown in Figure 1, a and b, respectively, are similar. The maximum difference between calculated and experimental ring carbon–carbon distances is 0.037 Å, and the calculated C═O and ring carbon–carbon bond distances for UQ_0 differ from experimental values by an average absolute magnitude of only 0.012 Å. This average difference is less than the conventional criterion for determining whether or not two experimental bond distances are identical (3 times the standard deviation in bond distances is $3\sigma = 0.021$ Å in this case), so the calculated C═O and ring carbon–carbon bond distances of UQ_0 agree well with the X-ray diffraction distances. For UQ_0, one carbon–oxygen torsional angle places a methoxy carbon 10.6° above the ring plane, compared with 3.2° in the X-ray structure. The second methoxy group torsional angle of UQ_0 is calculated as 122.8°, whereas the experimental structure places this methoxy at −112.7°, below the plane in Figure 1a. We calculate, however, a second local minimum energy torsional angle of −123.6°, only 10^{-4} kcal/mol higher in energy than the global minimum and only 11° different from the experimental torsional angle. We also note that the X-ray diffraction structure of a 2,3-dimethoxy-5-prenyl-*p*-benzoquinone[39] shows the corresponding methoxy group with a torsional angle of 120.2°, very similar to that calculated for UQ_0. Although the near coplanarity of one methoxy substituent and the quinone ring may initially appear surprising, it is consistent with quantum chemical calculations for 2-methoxy-*p*-benzoquinone[40] and 2,6-dimethoxy-*p*-benzoquinone,[41] indicating significant π-electron delocalization from one methoxy oxygen to the quinone ring. So, even though X-ray diffraction structures include the structural effects of packing forces absent from our calculations, our calculated structure of UQ_0 agrees well with the published X-ray diffraction structure.

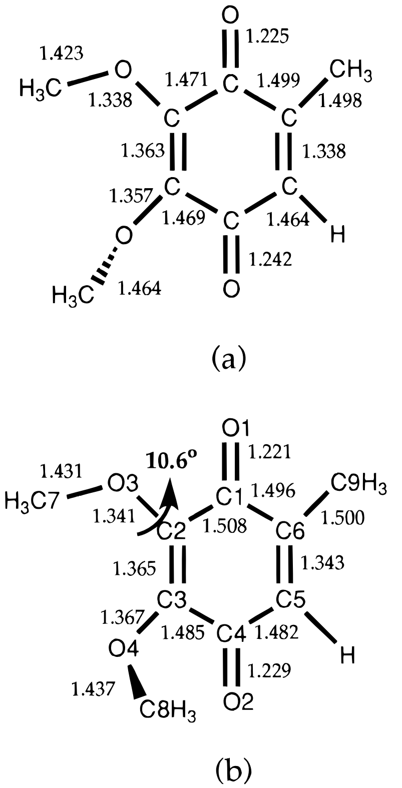

Figure 1. A comparison of bond distances (in Å) from (a) the X-ray diffraction structure of 2,3-dimethoxy-6-methyl-*p*-benzoquinone[38] and (b) B3LYP/6-31G(d) calculations for UQ_0. The atomic numbering scheme for UQ_0 is given in (b).

Figure 2a,b compares the calculated structures of UQ_1 and its radical anion, $UQ_1^{\bullet-}$. First, we note that the calculated bond distances of UQ_1 are extremely similar to those calculated for UQ_0 and shown in Figure 1b. The calculated C═O distances for the two molecules differ by less than 0.002 Å, whereas the ring carbon–carbon distances differ by an average absolute magnitude of only 0.005 Å and a maximum of 0.015 Å. Methoxy torsional angles are similarly close, with calculated values of 10.6° and 123° for the minimum-energy structure of UQ_0, compared with 9.7° and 122.8° for UQ_1. Like UQ_0, UQ_1 displays a second low-energy conformation, at −121° and 0.12 kcal/mol higher in energy than the global minimum.

Comparing the calculated structures of UQ_1 (Figure 2a) and $UQ_1^{\bullet-}$ (Figure 2b) shows several significant differences. First, reducing UQ_1 to $UQ_1^{\bullet-}$ lengthens calculated C═O bond distances by 0.047 and 0.040 Å, whereas the ring C═C bonds expand less, by 0.015 and 0.029 Å. In contrast, the ring C–C bonds all contract by amounts ranging from 0.025 to 0.048 Å. While these bond distance changes are qualitatively consistent with the nodal structure of *p*-benzosemiquinone radical anion's singly occupied molecular orbital,[1,42,43] geometrical changes within the methoxy substituents are also significant. Although one methoxy CC–OC torsional angle increases by only 2.1° upon reducing UQ_1, the second methoxy torsional angle shows a remarkably large change from 9.7° in UQ_1 to 123.2° in $UQ_1^{\bullet-}$. Apparently, reducing UQ_1 to $UQ_1^{\bullet-}$ forces *both* methoxy groups

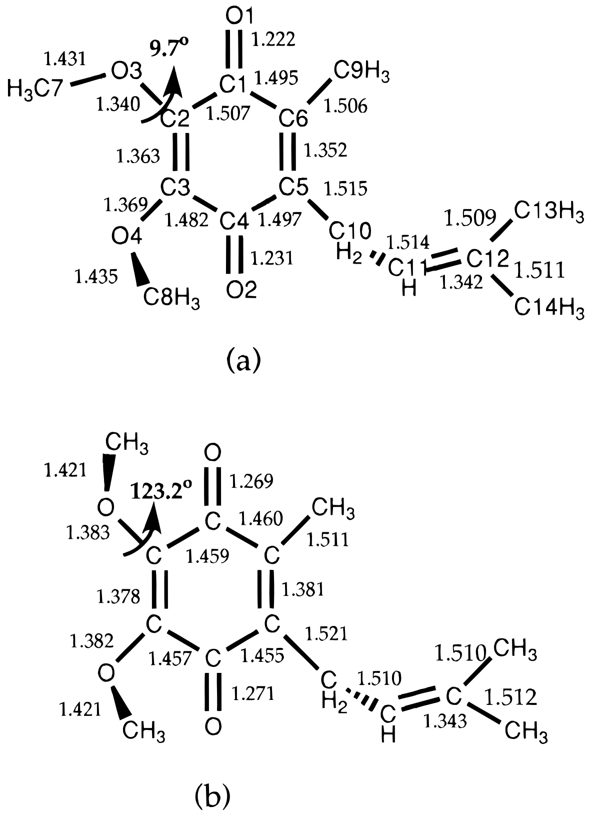

Figure 2. A comparison of calculated bond distances (in Å) for (a) UQ_1 and (b) $UQ_1^{\bullet -}$. The large torsional angle change for one methoxy group from UQ_1 (9.7°) to $UQ_1^{\bullet -}$ (123.2°) is also indicated. The atomic number scheme for UQ_1 is given in (a).

TABLE 1: Hyperfine Coupling Constants and Spin Densities for Ubisemiquinone-1 Radical Anion ($UQ_1^{\bullet -}$) Calculated by Using the B3LYP Hybrid Hartree−Fock Density Functional Method and 6-31G(d) and [632|41] Basis Sets

	hyperfine coupling constants			spin densities	
atom no.	6-31G(d)	[632|41]	exptl[a]	6-31G(d)	[632|41]
C1	+0.51	−2.15	−0.93	0.087	0.095
C2	+0.99	−0.46		0.060	0.078
C3	+0.58	−0.75	0.65−0.8	0.052	0.080
C4	+1.30	−1.53	1.5−1.6	0.097	0.094
C5	+1.45	−0.27		0.074	0.065
C6	+2.72	+0.40		0.101	0.072
C7	+0.24	+0.46		0.002	0.000
C8	+0.10	+0.29		0.001	0.000
C9	−1.60	−1.66	1.51−1.71	−0.011	−0.006
C_{10}	−1.23	−1.32		−0.008	−0.006
C11	+1.45	+1.66		0.003	0.007
C12	+0.17	+0.10		0.003	0.001
C_{13}	−0.04	−0.04		0.000	0.001
C_{14}	+0.10	+0.13		0.000	0.000
O_1	−8.67	−7.11		0.270	0.248
O_2	−8.06	−6.80		0.251	0.236
O_3	−0.77	−0.61		0.003	0.008
O_4	−0.65	−0.56		0.003	0.008
ave C_7 protons	−0.03	−0.02		0.000	0.000
ave C_8 protons	−0.03	−0.02		0.000	0.001
ave C_9 protons	+2.30	+2.24	2.09−2.20	0.003	0.004
ave C_{10} protons	+0.95	+0.95	1.04−1.06	0.001	0.002
C_{11} proton	−0.05	−0.08		−0.001	0.000
ave C_{13} protons	+0.03	+0.03		0.000	0.000
ave C_{14} protons	+0.06	+0.05		0.000	0.000

[a] Kropacheva, T. N.; van Liemt, W. B. S.; Raap, J.; Lugtenburg, J.; Hoff, A. J. *J. Phys. Chem.* **1996**, *100*, 10433−10442 and references therein. Samoilova, R. I.; Gritsan, N. P.; Hoff, A. J.; van Liemt, W. B. S.; Lugtenburg, J.; Spoyalov, A. P.; Tsvetkov, Y. D. *J. Chem. Soc., Perkin Trans. 2* **1995**, 2063.

to adopt conformations inappropriate for significant π-delocalization between their oxygen atoms and the quinone ring.

Table 1 compares calculated atomic spin densities and isotropic hyperfine coupling constants (hfcc's) for $UQ_1^{\bullet -}$, calculated by using two different basis sets, with experimentally derived hfcc's.[25,27,28] Values reported in the table were obtained by optimizing geometries with the 6-31G(d) basis set and performing a single-point calculation with the [632|41] basis at the 6-31G(d) geometry. The [632|41] basis set proposed by Chipman[44] was designed specifically to model spin properties of radicals and includes diffuse and polarization functions on heavy atoms, as well as a tighter s function on hydrogens. Hfcc's were determined from Fermi contact spin densities, $\rho(N)$, using the formula[31,32]

$$a_0 = [(8\pi/3)gg_N\beta\beta_N]\rho(N)$$

where a_0 is the hfcc (in gauss), g is the electronic g factor, β is the electronic Bohr magneton, and g_N and β_N are the analogous values for nucleus N. The term in brackets can be expressed as a single factor (in units of gauss) for each type of nucleus: 1595 for ^1H, 401.0 for ^{13}C, and −216.2 for ^{17}O. Here, we emphasize results obtained with the [632|41] basis set, because it was designed to reproduce spin properties of radicals accurately.

The largest calculated spin density appears on O1 (0.248), the carbonyl oxygen *meta* to the isoprenyl chain, with only slightly lower spin density on O2 (0.236), located *ortho* to the same chain. Calculated spin densities on the quinoidal oxygens agree qualitatively with the spin density inferred from magnetic resonance experiments with ^{17}O labeling (0.21).[26] Among the carbon atoms, the largest spin density is apparently on the carbonyl carbons C1 (0.095) and C4 (0.094), slightly lower spin density appears on the methoxy-bearing carbons C2 (0.078) and C3 (0.080), and the spin density on C5 (0.065) and C6 (0.072) is very slightly lower. A tiny amount of unpaired electron spin appears on the methoxy, methyl, and isoprenyl side chains. Although the relative spin densities for carbon atoms C1 > C4 > C3 > C2 > C6 > C5 are intuitively correct, they should be viewed with caution since differences are small and their relative magnitudes depend on the specific basis set used.

Isotropic hyperfine coupling constants (hfcc's) roughly parallel the calculated atomic spin densities, with large hyperfine coupling constants for atoms carrying high spin densities. Exceptions are the side chain carbons C9, C10, and C11 and the hydrogens on C9 and C10, atoms that carry very little spin density but display significant hyperfine couplings. Comparing calculated hyperfine coupling constants with available experimental values in the aprotic solvent DME[25,27,28] shows excellent agreement. Specifically, the C9 methyl protons have a calculated, average hfcc of 2.24 (experimental values range from 2.09 to 2.20), and the average calculated hfcc for the C10 methylene protons is 0.95 (experimental values are 1.04 and 1.06).[25,28] Heavy atom hfcc's are generally more difficult to calculate than proton hfcc's, yet the largest error in the calculated $^{13}C1$ hfcc (−2.15) is only 1.22 (the experimental hfcc is −0.93). For C3, C4, and C9, on the other hand, the calculated ^{13}C hfccs (−0.75 for C3, −1.53 for C4, and −1.66 for C9) are all within the range of experimentally determined magnitudes of hfcc's for UQ_0 (0.65−0.8 for C3, 1.5−1.6 for C4, and 1.51−1.71 for C9).[27] We note that calculated heavy atom hfcc's are extremely sensitive to the size of the basis set, so the overall agreement between the magnitudes of calculated and experimental hfcc's is excellent.

Table 2 lists unscaled, calculated vibrational frequencies for UQ and $UQ^{\bullet -}$ for comparison with available experimental

TABLE 2: Approximate Mode Descriptions and Unscaled Vibrational Frequencies for a Model of Ubiquinone-1 (UQ) and Ubisemiquinone-1 Anion ($UQ^{\bullet -}$) Calculated by Using the B3LYP Hybrid Hartree−Fock/Density Functional Method and a 6-31G(d) Basis Set

mode	approx description	UQ	$UQ^{\bullet -}$
84	C−H stretch (chain)	3236	3209
83	C−H stretch (methoxy)	3177	3136
82	C−H stretch (methoxy)	3175	3137
81	C−H stretch (chain)	3171	3165
80	C−H stetch (methyl)	3170	3139
79	C−H stretch (chain)	3154	3134
78	C−H stretch (methoxy)	3147	3079
77	C−H stretch (methoxy)	3136	3078
76	C−H stretch (methyl, chain)	3112	3059
75	C−H stretch (methyl, chain)	3107	3033
74	C−H stretch (methoxy, chain)	3064	3081
73	C−H stretch (methoxy, chain)	3064	2947
72	C−H stretch (methyl)	3051	3009
71	C−H stretch (methoxy)	3035	2989
70	C1−O1 stretch	1751 (1664)	1552 (1486)
69	C11−C12 stretch	1725	1717
68	C4−O2 stretch	1715 (1644)	1542 (1466)
67	C2−C3/C5−C6 stretch (sym)	1710	1654 (1617)
66	C2−C3/C5−C6 str (asym)	1663 (1614)	1556 (1527)
65	C−H bd (methoxy)	1544	1553
64	C−H bd (methyl)	1528	1535
63	C−H bd (methoxy)	1523	1508
62	C−H bd (methoxy)	1518	1505
61	C−H bd (methyl)	1516	1516
60	C−H bd (methoxy)	1513	1509
59	C−H bd (methoxy)	1507	1506
58	C−H bd (chain)	1497	1488
57	C−H bd (methoxy)	1481	1467
56	C−H bd (chain)	1470	1466
55	C−H bd (methyl)	1430	1401
54	chain stretch/torsion	1356	1339
53	chain torsion	1340	1313
52	ring stretch/bend	1335	1304
51	chain torsion	1324	1273
50	ring stretch/bend	1299	1258
49	chain torsion	1271	1273
48	methoxy bd	1234 (1288)	1227
47	methoxy bd	1228 (1266)	1223
46	ring stretch	1191	1194
45	methoxy twisting	1177	1194
44	methoxy twisting	1174	1181
43	chain/ring torsion	1157	1179
42	ring stretch/bend	1131	1134
41	methyl/ring torsions	1096	1161
40	methyl bd	1062	1064
39	ring breathing/chain torsion	1049	1061
38	ring bd/chain torsion	1036	1046
37	ring bd/C−O stretch	976	999
36	methyl bd/ring torsion	960	967
35	ring torsion	954	946
34	chain torsion	938	919
33	C═O bd	920	901
32	C═O bd	886	751
31	C═O bd	759	750
30	ring torsion	766	727
29	C═O bd	729	712
28	ring deformation	702	695
27	ring deformation	611	633
26	ring bending	592	584
25	ring breathing	541	557
24	ring torsion	503	501
23	ring bd	460	472
22	C═O bd	445	440
21	ring bd/torsion	435	414
20	C═O bd	403	401
19	chain torsion/C═O bd	384	381
18	COC bd	352	356
17	COC bd	342	344
16	ring-methyl/COC bd	328	331
15	ring-methyl/COC bd	294	301
14	ring bd	280	292
13	COC bd	231	251
12	methoxy rotation	223	158
11	methoxy wag/rotation	203	207
10	chain torsion/methoxy rotation	175	178
9	methoxy rotation	136	174
8	methyl rotation	121	130
7	chain torsion/methoxy rotation	105	128
6	methoxy torsions	97	100
5	methoxy torsions	93	80
4	C═O wag/chain torsion methoxy torsion	71	99
3	chain torsion	58	84
2	chain-ring bd	37	56
1	chain-ring bd	30	36

data.[19−24] Although some workers scale calculated vibrational frequencies by a multiplicative factor to bring them into better agreement with experiment and scaling factors appropriate for B3LYP-derived frequencies (0.963, 0.9614) have been determined,[45,46] we prefer to report unscaled frequencies. We focus on C═O stretching, ring C═C stretching, and methoxy frequencies because these frequencies have been experimentally measured and are key to inferences concerning the influence of the protein on ubiquinone structures. For neutral UQ, the mode calculated at 1751 cm^{-1} is a stretching vibration concentrated at the C═O bond *meta* to the isoprenoid chain and corresponds most closely to the recently observed UQ_1 C═O stretching mode at 1664 cm^{-1}.[19] The 1715 cm^{-1} UQ mode is a C═O stretch concentrated on the C═O bond *ortho* to the isoprenoid chain and agrees with the assignment for the band observed at 1644 cm^{-1} for UQ_1.[19] In contrast to the C═O stretching modes, the ring C═C stretches mix to form symmetric and antisymmetric modes involving both C═C bonds. The UQ vibration calculated at 1710 cm^{-1} nearly overlaps one calculated C═O band and represents the symmetric C═C stretching mode, while the 1663 cm^{-1} vibration is the antisymmetric C═C stretch. Although the lower frequency C═C stretch matches experimental assignments,[19,22−24] experiments typically detect only one C═C stretching band.[23,24] We therefore propose that the higher frequency, symmetric C═C stretch is indistinguishable because it nearly overlaps the lower frequency C═O stretching mode. Since the calculated IR intensity of the symmetric C═C stretch is one-fourth to one-fifth the intensities of the C═O stretches, and one-seventh the intensity of the antisymmetric C═C stretch, the symmetric C═C stretch is relatively difficult to distinguish in the infrared spectrum. To test the prediction that the symmetric C═C stretch overlaps one C═O stretching band, we would therefore suggest isotopic substitution experiments to shift either the C═O or C═C stretching mode out of their common frequency range, perhaps coupled with Raman or resonance Raman spectroscopy to enhance the intensity of the symmetric C═C stretch. The $C-O-CH_3$ bending modes are calculated at 1234 and 1228 cm^{-1}. The calculated frequencies are somewhat lower than the experimentally observed $C-O-CH_3$ bending modes at 1288 and 1266 cm^{-1} for UQ_1 and appear substantially mixed, in contrast with the experimental inference that the higher frequency $C-O-CH_3$ bending mode corresponds to the methoxy group in the plane of the ring.[16] Finally, the methoxy torsional modes appear at very low frequencies, 97 and 93 cm^{-1}. Each torsional mode is localized at one methoxy substituent, with the mode at 97 cm^{-1} involving torsions of the methoxy group *para* to the isoprenoid chain.

The primary differences in the calculated vibrations of the neutral UQ molecule and $UQ^{\bullet -}$ lie in the lower frequencies for the anion vibrations, the order of the C═O and ring C═C stretching frequencies, and the increased mixing between the modes of $UQ^{\bullet -}$. In the neutral molecule, the C═O modes are predicted at higher frequencies than the C═C stretches, while in the radical anion, the C═C modes are higher. Although the extent of mixing between C═O and C═C modes of the same symmetries make assignments difficult, a similar reversal in relative ordering of the C═O and C═C frequencies was also calculated for other *p*-benzoquinone/*p*-benzosemiquinone anion pairs.[47,48] In fact, the identical ordering—C═O stretching frequencies above the C═C stretching bands—was calculated for *p*-chloranil and *p*-fluoranil, while their anions showed calculated C═C stretching frequencies above C═O stretches. For the neutral *p*-benzoquinone, the C═O stretching modes are also calculated at higher frequencies than the C═C stretches, but for the corresponding anion the frequencies of the two C═C stretches bracket the calculated C═O stretching frequencies. Hence, in $UQ^{\bullet -}$ the C═C symmetric stretching vibration is calculated at 1654 cm^{-1} and the antisymmetric C═C stretch appears at 1566 cm^{-1}. The calculated frequencies are more accurate than expected from the B3LYP method and differ by approximately 2% from C═C stretching frequencies of 1617 and 1527 cm^{-1} experimentally measured for $UQ_1^{\bullet -}$.[22] Next in frequency is the antisymmetric C═O stretch calculated at 1552 cm^{-1}, followed by the symmetric C═O stretching mode at 1542 cm^{-1}. Although experiments imply that the C═O stretching modes of $UQ_1^{\bullet -}$ appear at 1486 and 1466 cm^{-1}, both C═O stretching modes were observed in the range from 1482 to 1500 cm^{-1} for $UQ_0^{\bullet -}$ and $UQ_{10}^{\bullet -}$.[19,23,24] We should also note that the C═O stretching modes of $UQ^{\bullet -}$ (1552 and 1542 cm^{-1}) are calculated to appear at nearly the same frequencies as several CH bending modes (1553 and 1535 cm^{-1}). As a result, deuterium isotopic substitution of methoxy and/or methyl hydrogens to shift CH bending frequencies may be necessary to pinpoint the C═O stretching modes experimentally. Finally, the methoxy torsional vibrations are mixed and appear distributed over three modes, at 100, 99, and 80 cm^{-1}.

Conclusions

This contribution presents calculated geometries and spin properties for ubiquinone-1 (UQ_1) and its radical anion ($UQ_1^{\bullet -}$), as well as vibrational frequencies for a model with the methyl groups on the isoprenyl side chain of UQ_1 replaced by hydrogens (UQ and $UQ^{\bullet}$). Computations were done by using the hybrid Hartree−Fock/density functional B3LYP method[29,30] with two different basis sets. Although more sophisticated computational methods, larger basis sets, and more realistic models will undoubtedly improve on the results presented here, this work makes a compromise between computational economy and rigor to provide several important, experimentally testable predictions.

Despite the absence of packing effects present in X-ray diffraction structures, the calculated geometry of UQ_1 agrees well with the calculated and X-ray diffraction[38] structures for UQ_0 (and with recently published calculations for UQ[15]). Furthermore, bond distance changes upon reducing UQ_1 to $UQ_1^{\bullet -}$ are qualitatively consistent with predictions based on calculations for other *p*-benzoquinones.[1,42,43,47,49,50] Reducing UQ_1 to $UQ_1^{\bullet -}$ also results in a large change of nearly 114° in the torsional angle calculated for the methoxy group located *para* to the isoprenyl chain.

Density functional and especially hybrid Hartree−Fock/density functional methods represent some of the most accurate, economical methods currently available for estimating spin properties of *p*-benzoquinones.[47−51] Calculated isotropic hyperfine coupling constants for the protons of $UQ_1^{\bullet -}$ agree well with experiment and reflect the radical's qualitative spin density distribution. With the exception of C1, the magnitudes of all calculated heavy atom hfcc's fall within a narrow range of experimentally determined values for several different ubiquinones. Thus, the overall agreement between calculated and experimental spin properties is excellent.

Unscaled, calculated C═O and ring C═C stretching vibrational frequencies for both UQ and $UQ^{\bullet -}$ also agree qualitatively with experiment. Calculated shifts in C═O stretching frequencies upon reducing UQ to $UQ^{\bullet -}$ (−191 and −167 cm^{-1}) are within 22 cm^{-1} of those observed experimentally (−169 and −160 cm^{-1}). Only one calculated shift in ring C═C stretching frequencies for $UQ^{\bullet -}$ relative to UQ (54 and 93 cm^{-1}) agrees with the experimentally measured shift (7 and 83 cm^{-1}), but for good reason. According to our calculations for UQ, the unresolved ring C═C stretch of UQ_1 has very low intensity in the IR spectrum and should lie very near one C═O stretch (C═O stretch, 1715/1710 cm^{-1}; C═C stretch, 1647 cm^{-1}) rather than overlapping the second C═C stretch measured at 1614 cm^{-1}. Our prediction concerning the location of the second C═C stretch may be tested by two isotopic substitution experiments to shift the C═O and then the C═C stretching modes out of their common frequency range. In addition, our calculations imply that the C═O stretching modes of $UQ^{\bullet -}$ (1552 and 1542 cm^{-1}) appear at nearly the same frequencies as several CH bending modes (1553 and 1535 cm^{-1}). As a result, deuterium isotopic substitution of methoxy and/or methyl hydrogens to shift CH bending frequencies may be useful to pinpoint the C═O stretching modes of $UQ^{\bullet -}$ accurately. Finally, calculated $C-O-CH_3$ bending frequencies for UQ appear substantially lower in frequency than experimentally measured bands assigned to these modes.

Acknowledgment. The research discussed in this publication was made possible by OCAST Award H97-091 from the Oklahoma Center for the Advancement of Science and Technology and by supercomputer time grants from the NSF/MetaCenter Allocations Committee, the NSF/National Center for Supercomputing Applications, and the NSF/Cornell Theory Center. The Cornell Theory Center receives major funding from the NSF and New York State. Additional funding comes from ARPA, the NIH, IBM Corp., and other members of the center's Corporate Research Institute. We are also grateful for supercomputer time at the University of Oklahoma made possible by support from IBM Corp., Silicon Graphics Inc., and the University of Oklahoma.

Supporting Information Available: Atom numbering systems and optimized geometries of ubiquinine-1 (UQ_1), the model 5-allyl-2,3-dimethoxy-1,4-benzoquinone (UQ_1 with isoprenyl methyl groups replaced by hydrogens, abbreviated UQ), and their radical anions ($UQ_1^{\bullet -}$ and $UQ^{\bullet -}$) obtained from B3LYP/6-31G(d) calculations (9 pages). Ordering information is given on any current masthead page.

References and Notes

(1) Boesch, S. E. M. S. Thesis, The University of Oklahoma, 1996.
(2) *Coenzyme Q. Biochemistry, Bioenergetics and Clinical Applications of Ubiquinone*; Lenaz, G., Ed.; Wiley-Interscience: Chichester, 1985.
(3) *Function of Quinones in Energy Conserving Systems*; Trumpower, B. L., Ed.; Academic: New York, 1982.
(4) Shinkarev, V. P.; Wraight, C. A. In *The Photosynthetic Reaction Center*; Deisenhofer, J., Norris, J. R., Eds.; Academic: San Diego, 1993; Vol. I, pp 193−255.
(5) Collins, M. D.; Jones, D. *Microbiol. Rev.* **1981**, *45*, 316−354.
(6) Brandt, U.; Trumpower, B. *Crit. Rev. Biochem. Mol. Biol.* **1994**, *29*, 165−197.
(7) Trumpower, B. L.; Gennis, R. B. *Annu. Rev. Biochem.* **1994**, *63*, 675−716.

(8) *Free Radicals and Antioxidants in Nutrition*; Corongiu, F., Banni, S., Dessi, M. A., Rice-Evans, C., Eds.; Richelieu Press: London, 1993.

(9) Deisenhofer, J.; Epp, O.; Sinning, I.; Michel, H. *J. Mol. Biol.* **1995**, *246*, 429−457.

(10) Lancaster, C. R. D.; Ermler, U.; Michel, H. In *Anoyxgenic Photosynthetic Bacteria*; Blankenship, R. E., Madigan, M. T., Bauer, C. E., Eds.; Kluwer: Dordrecht, 1995; pp 503−526.

(11) Ermler, U.; Fritzsch, G.; Buchanan, S. K.; Michel, H. *Structure* **1994**, *2*, 925−936.

(12) El-Kabbani, O.; Chang, C.-H.; Tiede, D.; Norris, J.; Schiffer, M. *Biochemistry* **1991**, *30*, 5361−5369.

(13) Allen, J. P.; Feher, G.; Yeates, T. O.; Komiya, H.; Rees, D. C. *Proc. Natl. Acad. Sci. U.S.A.* **1988**, *85*, 8487−8491.

(14) Allen, J. P.; Feher, G.; Yeates, T. O.; Komiya, H.; Rees, D. C. *Proc. Natl. Acad. Sci. U.S.A.* **1987**, *84*, 5730−5734.

(15) Nonella, M.; Brändl, C. *J. Phys. Chem.* **1996**, *100*, 14549−14559.

(16) Breton, J.; Nabedryk, E. *Biochim. Biophys. Acta* **1996**, *1275*, 84−90 and references therein.

(17) Mäntele, W. In *Anoyxgenic Photosynthetic Bacteria*; Blankenship, R. E., Madigan, M. T., Bauer, C. E., Eds.; Kluwer: Dordrecht, 1995; pp 627−647.

(18) Angerhofer, A.; Bittl, R. *Photochem. Photobiol.* **1996**, *63*, 11−38 and references therein.

(19) Burie, J.-R.; Boussac, A.; Boullais, C.; Berger, G.; Mattioli, T.; Mioskowski, C.; Nabedryk, E.; Breton, J. *J. Phys. Chem.* **1995**, *99*, 4059−4070.

(20) Breton, J.; Burie, J.-R.; Berthomieu, C.; Berger, G.; Nabedryk, E. *Biochemistry* **1994**, *33*, 4953−4965.

(21) Brudler, R.; de Groot, H. J. M.; van Liemt, W. B. S.; Steggerda, W. F.; Esmeijer, R.; Gast, P.; Hoff, A. J.; Lugtenburt, J.; Gerwert, K. *EMBO J.* **1994**, *13*, 5523−5530.

(22) Parker, A. W.; Hester, R. E.; Phillips, D.; Umapathy, S. *J. Chem. Soc., Faraday Trans.* **1992**, *88*, 2649−2653.

(23) Bauscher, M.; Mäntele, W. *J. Phys. Chem.* **1992**, *96*, 11101−11108.

(24) Bauscher, M.; Nabedryk, E.; Bagley, K.; Breton, J.; Mäntele, W. *FEBS Lett.* **1990**, *261*, 191−195.

(25) Kropacheva, T. N.; van Liemt, W. B. S.; Raap, J.; Lugtenburg, J.; Hoff, A. J. *J. Phys. Chem.* **1996**, *100*, 10433−10442 and references therein.

(26) MacMillan, F.; Lendzian, F.; Lubitz, W. *Magn. Reson. in Chem.* **1995**, *33*, S81−S93.

(27) Samoilova, R. I.; Gritsan, N. P.; Hoff, A. J.; van Liemt, W. B. S.; Lugtenburg, J.; Spoyalov, A. P.; Tsvetkov, Y. D. *J. Chem. Soc., Perkin Trans. 2* **1995**, 2063.

(28) Das, M. R.; Connor, H. D.; Leniart, D. S.; Freed, J. H. *J. Am. Chem. Soc.* **1970**, *92*, 2258−2268.

(29) Stephens, P. J.; Devlin, F. J.; Chablowski, C. F.; Frisch, M. J. *J. Phys. Chem.* **1994**, *98*, 11623−11627.

(30) Frisch, M. J.; Trucks, G. W.; Schlegel, H. B.; Gill, P. M. W.; Johnson, B. G.; Robb, M. A.; Cheeseman, J. R.; Keith, T. A.; Petersson, G. A.; Montgomery, J. A.; Raghavachari, K.; Al-Laham, M. A.; Zakrzewski, V. G.; Ortiz, J. V.; Foresman, J. B.; Cioslowski, J.; Stefanov, B. B.; Nanayakkara, A.; Challacombe, M.; Peng, C. Y.; Ayala, P. Y.; Chen, W.; Wong, M. W.; Andres, J. L.; Replogle, E. S.; Gomperts, R.; Martin, R. L.; Fox, D. J.; Binkley, J. S.; Defrees, D. J.; Baker, J.; Stewart, J. J. P.; Head-Gordon, M.; Gonzalez, C.; Pople, J. A. *GAUSSIAN94 (Revisions B.2, B.3, D.1, and D.2)*; Gaussian, Inc.: Pittsburgh, PA, 1995.

(31) Weil, J.; Bolton, J. R.; Wertz, J. E. *Electron Paramagnetic Resonance*; Wiley-Interscience: New York, 1994.

(32) Gordy, W. *Theory and Applications of Electron Spin Resonance*; Wiley-Interscience: New York, 1980.

(33) Mulliken, R. S. *J. Chem. Phys.* **1955**, *23*, 1833−1840.

(34) Pulay, P.; Torok, F. *Acta Chim. Acad. Sci. Hung.* **1965**, *47*, 273−279.

(35) Dupuis, M.; Spangler, D.; Wendoloski, J. J. *National Resource for Computations in Chemistry Catalog, Program QG01*; University of California: Berkeley, 1980.

(36) Schmidt, M. W.; Baldridge, K. K.; Boatz, J. A.; Jensen, J. H.; Koseki, S.; Gordon, M. S.; Nguyen, K. A.; Windus, T. L.; Elbert, S. T. *QCPE Bull.* **1990**, *10*, 52.

(37) Wasikowski, C.; Klemm, S. “XMOL Version 1.3.1,” Research Equipment, Inc. d.b.a. Minnesota Supercomputer Center, Inc., 1993.

(38) Silverman, J.; Stam-Thole, I.; Stam, C. H. *Acta Crystallogr. B* **1971**, *27*, 1846−1851.

(39) Schmalle, H. W.; Jarchow, O. H.; Hausen, B. M.; Schulz, K.-H. *Acta Crystallogr. C* **1984**, *40*, 1090−1092.

(40) Prince, R. C.; Halbert, T. R.; Upton, T. H. In *Advances in Membrane Biochemistry and Bioenergetics*; Plenum: New York, 1987.

(41) Robinson, H. H.; Kahn, S. D. *J. Am. Chem. Soc.* **1990**, *112*, 4728−4731.

(42) Wheeler, R. A. *J. Phys. Chem.* **1993**, *97*, 1533−1537.

(43) Boesch, S. E.; Wheeler, R. A. *J. Phys. Chem.* **1995**, *99*, 8125−8134.

(44) Chipman, D. M. *Theor. Chim. Acta* **1989**, *76*, 73−84. The basis set was obtained from the Extensible Computational Chemistry Environment Basis Set Database, Version 1.0, as developed and distributed by the Molecular Science Computing Facility, Environmental and Molecular Sciences Laboratory, which is part of the Pacific Northwest Laboratory, P.O. Box 999, Richland, WA 99352, and funded by the U.S. Department of Energy. The Pacific Northwest Laboratory is a multiprogram laboratory operated by Battelle Memorial Institute for the U.S. Department of Energy under Contract DE-AC06-76RLO 1830. Contact David Feller, Karen, Schuchardt, or Don Jones for further information.

(45) Rauhut, G.; Pulay, P. *J. Phys. Chem.* **1995**, *99*, 3093−3100.

(46) Scott, A. P.; Radom, L. *J. Phys. Chem.* **1996**, *100*, 16502−16513.

(47) Grafton, A. K.; Boesch, S. E.; Wheeler, R. A. *J. Mol. Struct.: THEOCHEM* **1997**, *392*, 1−11.

(48) Boesch, S. E.; Wheeler, R. A. *J. Phys. Chem. A*, submitted.

(49) Wise, K. E.; Grafton, A. K.; Wheeler, R. A. *J. Phys. Chem. A* **1997**, *101*, 1160−1165.

(50) Grafton, A. K.; Wheeler, R. A. *J. Phys. Chem. A*, in press.

(51) O’Malley, P. J.; Collins, S. J. *Chem. Phys. Lett.* **1996**, *259*, 296−300.